Identification of novel activity-dependent human *BDNF* transcripts

S.T. Munshi[1], A.A. Martin[1], C. Bouwkamp[1], G. van Woerden[2], B. Lendemeijer[1], N. Günhanlar[1], A.J.A. Kievit[3], Y. Elgersma[2], V. Bonifati[3], F.M.S. de Vrij[1#], S.A. Kushner[1#]

[1]*Dept of Psychiatry, Erasmus MC, Wytemaweg 80, 3015 CN Rotterdam, the Netherlands*

[2]*Dept of Neuroscience, Erasmus MC, Wytemaweg 80, 3015 CN Rotterdam, the Netherlands*

[3]*Dept of Clinical Genetics, Erasmus MC, Wytemaweg 80, 3015 CN Rotterdam, the Netherlands*

[#]*Both authors contributed equally*

Manuscript in preparation

ABSTRACT

The brain-derived neurotrophic factor (*BDNF*) gene exhibits high evolutionary conservation. However, the genomic architecture of human *BDNF* is structurally and functionally more complex than in non-primate species. Few studies have investigated the transcriptional regulation of the human *BDNF* gene. Here, we demonstrate that human *BDNF* exon VIII-containing transcripts are strongly upregulated upon depolarization in multiple neural lineage cell types, most notably neural progenitor cells. Additionally, we identify three previously unreported *BDNF* exon VIII-containing transcripts (*BDNF* IV-VIII-IX, *BDNF* VIa-VIII-IX, *BDNF* VIb-VIII-IX,) that are not detected in mice, thereby bringing to 20 the total number of human *BDNF* transcripts identified to date. Lastly, we ascertained a previously unreported family with a Mendelian pattern of schizophrenia inheritance segregating a 2-basepair frameshift deletion within the coding sequence of exon VIII, providing support for the functional relevance of human *BDNF* exon VIII-containing transcripts. Our findings provide novel insight into the genomic architecture and transcriptional regulation of the human *BDNF* gene.

INTRODUCTION

Brain-derived neurotrophic factor (*BDNF*) is a fundamental regulator of brain development facilitating proliferation, differentiation, axonal and dendritic outgrowth, synaptogenesis, synaptic functioning and plasticity of neurons[1–3]. There is considerable evidence that human BDNF dysregulation is related to neurological and psychiatric disorders[4–9].

The human *BDNF* gene is highly complex which is reflected in the existence of multiple promoters, expression of multiple transcripts through alternative splicing and polyadenylation patterns, and synthesis of several BDNF protein precursor isoforms. The majority of prior studies on *BDNF* transcriptional regulation have been performed in rodent species, particularly *Mus musculus* (mouse) and *Rattus norvegicus* (rat). The human *BDNF* gene however has distinct features from rodent *Bdnf* (**Figure 1a)**. The rodent *Bdnf* gene has 9 exons, while human *BDNF* has 11 exons. Thus far, 17 alternatively-spliced human *BDNF* transcripts have been reported (**Figure 1b**)[10], whilst in both mouse and rat, 11 transcripts have been recognized. The majority of the transcripts are bipartite, containing a non-translating 5' exon spliced to a coding common-for-all 3' exon. Most known transcripts code for the same pro-BDNF protein, except transcripts I-IX in mouse and rats, and transcripts I-IX, VIIb-IX and VIII-IX in humans. Because of an in-frame translation start site, these transcripts allow production of an alternative longer protein called prepro-BDNF (**Figure 1c**).

The human *BDNF* VIII-IX transcript is a particular exception, as translation of this transcript is predicted to lead to a prepro-BDNF protein with a significantly longer alternative N-terminus. Interestingly, although exon VIII of rodent *Bdnf* also contains a homologous ATG, a nearby downstream 2-basepair deletion results in an intra-exonic stop codon that is out-of-frame for translation of mature BDNF (**Figure 1d**). The function of a potentially longer alternative N-terminus remains unknown. Recently, an independent ligand function for the pro-domain of BDNF was postulated[11,12].

In mouse and rat, transcript *BDNF* VIII-IX is expressed at low levels in the developing brain, but prominently present in different parts of the brain in adults[13]. Like many of the BDNF transcripts in mouse and rat, its expression is activity-dependent[13,14]. In humans however, few studies have reported detection of *BDNF* VIII-IX expression[10,15] which show contradicting findings. Additionally, the transcriptional regulation of human *BDNF* VIII-IX is completely unknown.

This study focuses on human *BDNF* exon VIII-containing transcripts. Making use of human pluripotent stem cell technology, we find that exon VIII-containing transcripts are upregulated upon depolarization in neural cells and most prominently in human neural progenitor cells. Additionally, we identified two novel human *BDNF* exon VIII-containing transcripts absent in mice. Also, we identified a 2-basepair frameshift deletion in the coding part of exon VIII that segregates with schizophrenia in a family with a Mendelian pattern of disease inheritance, in support of the functional relevance of *BDNF* human exon VIII-containing transcripts.

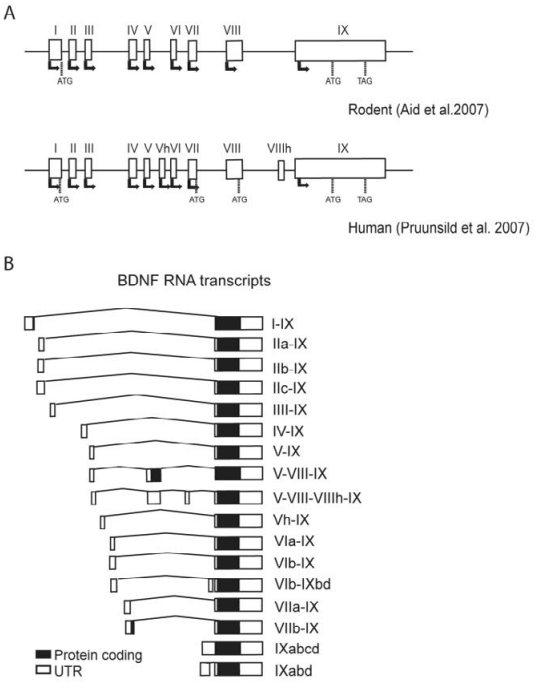

C

MFHQVRRVMTILFLTMVI start site in exon I
MQSREEWFHQVRRVMTILFLTMVI start site in exon VIIb
MCGATSFLHECTRLILVTTQNAEFLQKGLQVHTCFGVYPHASVWHDCASQKKGCAVYLHVSVEFNKLIPENGFIKFHQVRRVMTILFLTMVI start site in exon VIII
MTILFLTMVI start site in exon IX

D

```
Human BDNF  1    ACAGTTAAGTAATTAAAAGAAATTATAGAGTGGGATGCAAAAATAACCCGAAGGACAACT  60
Mouse BDNF  1    -ACAGTAAGCAATTAAAAGAAATTATAGAGTTGGATGCAAGCATAACCCGAAGGACAACT  59

Human BDNF  61   GGATGTGTGGAGCCACCAGTTTTCTCCATGAGTGCACAAGGTTAATCCTTGTTACTACTC  120
Mouse BDNF  60   GGATGTGTGGAACCACCAGTTTTCTCCATG--TGCTCAGGCTAATCCTCATTAATAACTC  117

Human BDNF  121  AGAATGCTGAGTTTCTACAGAAAGGGTTGCAGGTCCACACATGTTTTGGCGTCTACCCAC  180
Mouse BDNF  118  AGAAAGTTGAGTTTCTACAGAATGGGTTGCATGTCCATACATGTTTTGGCATCTACCCAC  177

Human BDNF  181  ACGCTTCTGTATGGCATGACTGTGCATCCCAGAAGAAGGGCTGTGCTGTGTACCTCCACG  240
Mouse BDNF  178  ACACTTTTATGTGGTATGACTGTGCATCCCAGGAGAAAGGCTGTGGTGTGTGTCGCTGCG  237

Human BDNF  241  TTTCAGTGGAATTTAACAAACTGATCCCTGAAAATGGTTTCATAAAGGTGA           291
Mouse BDNF  238  CCTCAGTGGAGCCGAACAAACTGATTGCTGAAAATGGTGTCGTAAAGGTGA           288
```

Figure 1. Characteristics of the *BDNF* gene. (A) Rodent and human *BDNF* gene structure. Human *BDNF* contains open-reading frames in exon VIb and VIII which are absent in mice and rats. (B) Alternative transcripts of human *BDNF*. (C) Amino acid sequences of different human prepro-BDNF N-termini. Amino acids encoded by exon IX are in grey and sequences encoded by alternative 5′ exons are in black (adapted from Pruunsild et al. 2007[16]). (D) Sequence alignment of mouse and human *BDNF* exon VIII. Human *BDNF* exon VIII contains an open-reading frame while mouse *BDNF* exon VIII contains an in frame stop-codon.

RESULTS

Human BDNF exon VIII transcription exhibits strong activity-dependent regulation

Human *BDNF* exon VIII-containing transcripts were first identified by Pruunsild et al. 2007[16]. Moreover, they reported that exon VIII was rarely identified in *BDNF* transcripts in the adult human brain. Because of BDNF's substantial involvement in neurodevelopment, we hypothesized that its appearance may be more prominent in developing neural lineages. We generated human neural progenitor cells (NPCs), neurons, and astrocytes from the H9 human embryonic stem cell (hESC) line (**Figure 2a**). Using qRT-PCR and exon-specific primers (**Table S2**) we detected *BDNF* transcripts spliced from exon VIII to IX (BDNF VIII-IX) at very low levels in all cell types examined. Since rodent *BDNF* is upregulated upon neuronal depolarization[17,18], we hypothesized that expression of human *BDNF* exon VIII-containing transcripts may be activity-dependent. Therefore we stimulated NPCs with varying concentrations of KCl to induce depolarization (**Figure 2b**). *BDNF* transcript levels were quantified by normalizing to *GAPDH*, which we confirmed was similar between depolarized and non-depolarized conditions (mean Ct treated cultures: 17.7 ± 0.2, mean Ct untreated cultures: 17.7 ± 0.2, Student *t*-test, p=0.54, n=3, 2 independent cultures). Compared to the Ctrl (4.2 mM) KCl concentration in the cell culture medium, *BDNF* exon VIII-containing transcripts were 10-fold and 48-fold upregulated in the 50 mM and 100 mM KCl condition, respectively (fold change 50 mM KCl: 10.5 ± 1.9, mean dCt treated cultures: 13.9 ± 0.3, mean dCt untreated cultures: 17.2 ± 0.3, Student *t*-test, p=1.2E-05; fold change 100 mM KCl: 48.5 ± 2.4, mean dCt treated cultures: 11.6 ± 0.1, mean dCt untreated cultures: 17.2 ± 0.3, Student *t*-test, p=2.8E-09). Total human *BDNF* levels (exon IX) were significantly upregulated in the 50 mM condition (mean relative fold change: 2.2 ± 0.3, mean dCt treated cultures: 8.7 ± 0.2, mean dCt untreated cultures: 9.7 ± 0.1, Student *t*-test, p<0.01). Together, these findings suggest that the transcription of human *BDNF* exon VIII is strongly activity-dependent.

We next sought to examine the activity-dependence of human *BDNF* exon VIII transcription in other neural lineage cell types. To allow for the possibility of observing increased or decreased transcript levels compared to NPCs, we proceeded with the intermediate 50 mM KCl concentration (**Figure 2c**). In baseline (4.2 mM) KCl, neurons and astrocytes exhibited similarly low levels of both total and exon VIII-containing *BDNF* transcripts. However, upon administration of 50 mM KCl, exon VIII-containing *BDNF* transcript levels were significantly upregulated in neurons (relative fold change: 9.8 ± 2.7, mean dCt treated cultures: 12.3 ± 0.4, mean dCt untreated cultures: 15.3 ± 0.3, Student *t*-test, p<0.001) and astrocytes (relative fold change: 10.3 ± 2.7, mean dCt treated cultures: 11.6 ± 0.6, mean dCt untreated cultures: 14.5 ± 0.2, Student *t*-test, p<0.001), whereas total *BDNF* levels were 2-fold (mean relative fold change: 1,9 ± 0.2, mean dCt treated cultures: 8.3 ± 0.1, mean dCt untreated cultures: 9.2 ± 0.1, Student *t*-test, p<0.001) and 3-fold (mean relative fold change: 3.0 ± 0.8, mean dCt treated cultures: 7.1 ± 0.5, mean dCt untreated cultures: 8.3 ± 0.4, Student *t*-test, p=0.06) upregulated in

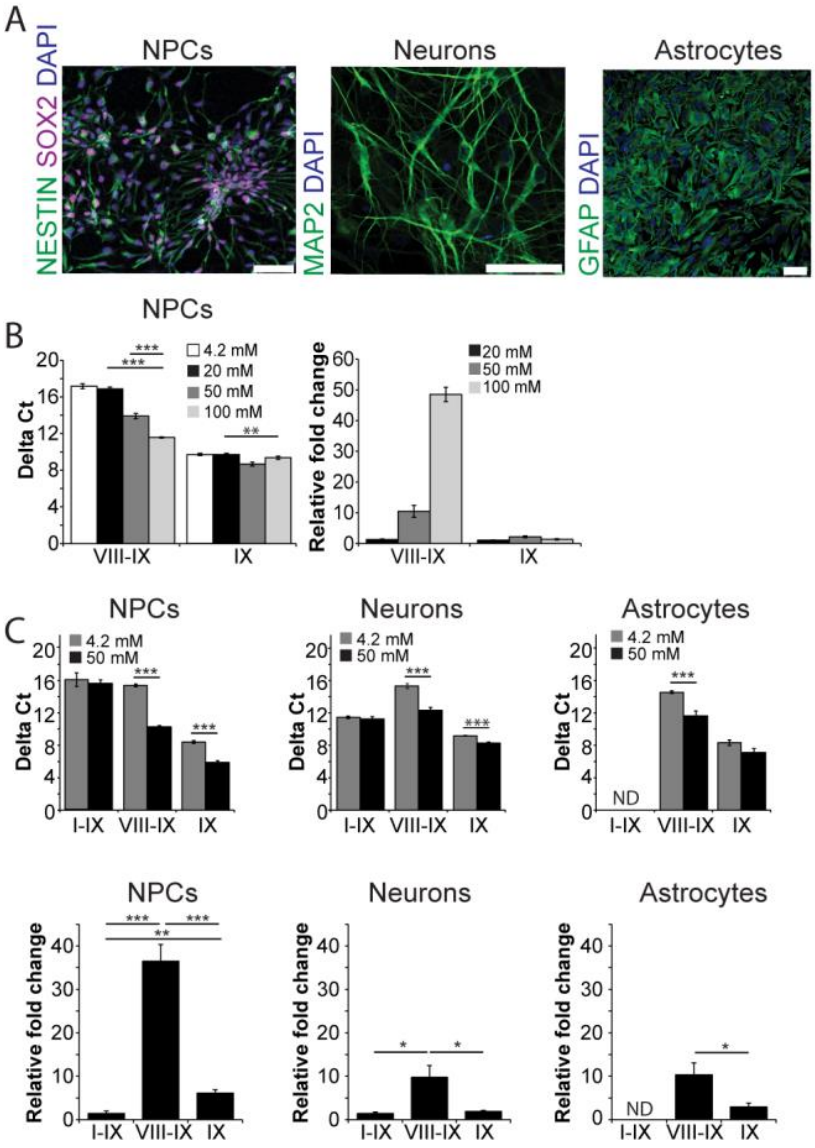

Figure 2. *BDNF* exon VIII is upregulated upon depolarization in human neural lineages. (A) Immunostainings of NPCs for SOX2 and nestin, and neurons for MAP2, and astrocytes for GFAP derived from H9 hESCs. Scale bars, 50 μm. (B) NPCs were treated for 3hs with 20 mM, 50 mM or 100 mM KCl and *BDNF* expression was measured by qRT-PCR using transcript-specific primers, normalized to *GAPDH* transcript levels. Delta Ct values and relative fold change values are shown. Relative fold change values are calculated with respect to untreated cultures. (C) NPCs, neuronal cultures and astrocytes were treated for 3hs with 50 mM KCl and *BDNF* expression was measured by qRT-PCR using transcript-specific primers, normalized to *GAPDH* transcript levels. Delta Ct and relative fold change values are shown. Relative fold change values are calculated with respect to untreated cultures. Error bars represent SEM. Statistical significance is denoted by asterisks (***p<0.001; **p<0.01; *p<0.05; NS; Student *t*-test, ANOVA).

neuronal cultures and astrocytes. The *BDNF* I-IX transcript, previously shown to be strongly upregulated in rodent neurons following depolarization[18–20], was not upregulated in human neurons following depolarization (mean dCt treated cultures: 11.3 ± 0.3, mean dCt untreated cultures: 11.5 ± 0.2, Student *t*-test, p=0.58) and was undetectable in human astrocytes.

In order to further validate our findings, we performed multiple additional replications. First, we repeated the quantification of *BDNF* VIII-IX levels with a new primer set containing no overlapping primer sequence compared to those originally used. Results using this additional primer pair was highly similar in all three neural lineage cell types to those obtained with the initial *BDNF* VIII-IX primers (**Figure S1a**). Second, we repeated the experiment using human iPSC-derived NPCs, which showed similar results as H9-derived cultures (**Figure S1b**), thereby confirming that our findings appear to be generalizable, at least among human pluripotent stem cell-derived neural progenitors. Third, in order to ensure that the observed activity-dependent upregulation of *BDNF* VIII-IX is not the result of excitotoxicity due to the administration of increased extracellular KCl, we exposed NPCs to 50 mM KCl for 3h and then replaced the culture medium with baseline (4.2 mM) KCl (**Figure S1c**). *BDNF* VIII-IX and total *BDNF* levels were measured at 3 and 18hs following medium replacement. *GAPDH* levels remained unchanged. Moreover, both *BDNF* VIII-IX and IX levels returned to baseline within three hours, thereby suggesting that upregulation of *BDNF* VIII-IX was not associated with excitotoxicity.

Taken together, transcriptional activation of *BDNF* exon VIII is strongly activity-dependent in multiple human neural lineage cell types, including neurons, astrocytes, and neural progenitors.

No evidence for activity-dependent regulation of mouse *Bdnf* exon VIII

The *Bdnf* VIII-IX transcript has been previously reported in mice[13]. However, it remains unknown whether activity-dependent regulation of human *BDNF* exon VIII is also observed for the mouse *Bdnf* gene. We exposed human ES-derived NPCs, mouse ES-derived NPCs, and mouse primary hippocampal neurons to 50 mM KCl for 3h. *BDNF* VIII-IX, I-IX, and IX transcript levels were robustly increased in human NPCs (**Figure 3a,b**). In contrast, *Bdnf* IX levels were decreased in mouse NPCs (mean relative fold change: 4.2 ± 0.2, mean dCt treated: 8.1 ± 0.1, mean dCt untreated: 6.1 ± 0.4, Student *t*-test, p<0.01), while *Bdnf* I-IX and VIII-IX transcripts were undetectable at baseline and following 50 mM KCl. Moreover, although *Bdnf* IX (mean relative fold change: 2.4 ± 0.6, mean dCt treated: 1.16 ± 0.3, mean dCt untreated: 2.3 ± 0.2, Student *t*-test, p<0.05) and *Bdnf* I-IX (mean relative fold change: 5.2 ± 2.3, mean dCt treated: 1.7 ± 0.5, mean dCt untreated: 3.6 ± 0.3, Student *t*-test, p<0.01) were upregulated in mouse primary hippocampal neurons following 50 mM KCl, *Bdnf* VIII-IX remained undetectable. Therefore, the robust activity-dependent regulation of human *BDNF* VIII-IX does not appear to extend to mice.

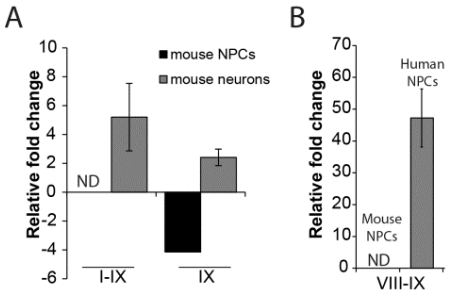

Figure 3. No detection of *BDNF* exon VIII in depolarized neural lineages of mice. (A, B) Mouse and human NPCs as well as primary mouse neurons were treated for 3hs with 50 mM KCl. *BDNF* expression was measured by qRT-PCR using transcript-specific primers. *BDNF* VIII-IX was measured using a primer pair that recognized mouse and human *BDNF* VIII-IX. Fold changes are relative to untreated cultures. Error bars represent SEM.

Identification of novel human *BDNF* exon VIII-containing transcripts

Pruunsild et al. 2007 reported human *BDNF* exon VIII to be contained within a tripartite transcript in which the transcriptional start site was exclusively contained within exon V[16]. Despite using multiple independent primer pairs for PCR and qPCR, we were unable to detect *BDNF* V-VIII-containing transcripts in human pluripotent stem cell-derived neural lineage cell types. Therefore, we designed primers to measure hypothetical transcripts starting from all possible upstream exons spliced to exon VIII. Using human NPCs, we found transcripts joining exon IV to exon VIII and exon VI to exon VIII (**Figure 4a**), both of which were upregulated following 50 mM KCl depolarization. Sanger sequencing of the PCR products confirmed that exons IV, and VI (VIa and VIb) each spliced to exon VIII. Next, we tested if these transcripts were also present in neuronal cultures and astrocytes. Upon depolarization with 50 mM KCl, all three exon VIII-containing transcripts (*BDNF* IV-VIII-IX, *BDNF* VIa-VIII-IX and *BDNF* VIb-VIII-IX) were upregulated in human NPCs, neuronal cells and astrocytes **(Figure 4b, Table S1).** These findings establish three activity-dependent human *BDNF* transcripts that to our knowledge have not been previously reported.

Candidate pathogenic variant in exon VIII segregating with the development of schizophrenia in a Dutch family

We ascertained a family of Dutch ancestry with a Mendelian pattern of inheritance for schizophrenia (SCZ) (**Figure 5**). No copy number variants were identified that segregated with the disease. Parametric linkage analysis under an autosomal dominant model yielded ~407 Mb of shared genomic regions (**Table S3**). Whole exome sequencing was performed in three individuals (**Figure 5**, PED IDs 1, 2, 5) at 100x average genomic coverage. The results of linkage analysis were used to filter the exome data for heterozygous variants within the genomic regions shared among the affected individuals. The resulting variants were filtered for those with minor allele frequency <0.1%, predicted to affect protein coding, called in both affected individuals while absent in the unaffected father, and absent from dbSNP129. In the resulting list of variants (**Table 1**), only one heterozygous variant stood out to potentially result in a severe loss-of-function, within a loss-of-function intolerant gene (pLI ≥ 0.9[21] in Exome Aggregation Consortium browser, ExAC)[22]: a frameshift mutation involving a 2-base

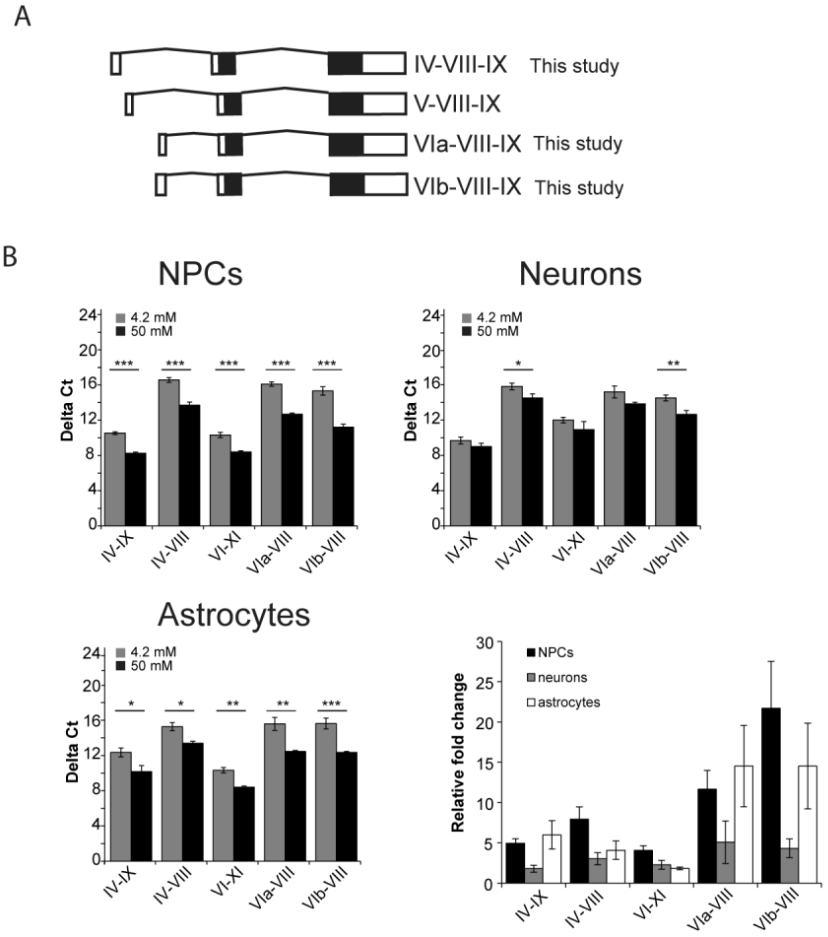

Figure 4. **Detection of novel, activity-dependent exon VIII-containing transcripts**. (A) Newly discovered *BDNF* transcripts in human neural lineages. (B) Human NPCs, neurons and astrocytes were treated for 3hs with 50 mM KCl. *BDNF* expression was measured by qRT-PCR using transcript-specific primers. Delta Ct and relative fold change values are shown. Relative fold change values are calculated with respect to untreated cultures. Error bars represent SEM. Statistical significance is denoted by asterisks (***p<0.001; **p<0.01; *p<0.05; NS; Student *t*-test, ANOVA).

pair deletion in *BDNF* exon VIII (Chr11:27,695,731-27,695,733, cDNA position c.99_100del2, p.Cys34PhefsTer12, **Table 1**). Sanger sequencing confirmed the presence of the mutation in all affected family members for whom DNA was available. In addition, one unaffected family member was also found to carry the same mutation, consistent with incomplete penetrance. We found the same mutation in the Swedish Schizophrenia Exome Sequencing Study (dbGAP; phs000473.v1.p1)[23] but the mutation was not enriched in cases vs controls (case:carriers 2536:0, control:carriers 2543:2, Fisher's Exact Test, p=0.4999.

Table 1, candidate variants in Dutch family with high incidence of schizophrenia.

Chr	Start	End	Gene	Ref	Alt	Zygosity	RS-number	cDNA	prot. pos.	Amino acid change	Mutation type	Amino acid change	Exac frequency (non-Finnish Europeans)	pLI score (ExAC)
11	27695731	27695733	BDNF	CAT	C	het	n/a	242	34	C34PhefsTer12	frameshift	C34PhefsTer12	0.0009052	0.95
4	1348905	1348905	UVSSA	C	T	het	n/a	1495	350	R350C	Nonsynonymous (missense,splicing)	R/C	1.55E-05	0.00
5	86703854	86703854	CCNH	T	G	het	rs199815978	689	155	N155T	Nonsynonymous (missense)	N/T	4.50E-05	0.00
8	17503464	17503464	MTUS1	A	G	het	rs202148873	1845	509	F509L	Nonsynonymous (missense)	F/L	0.0002013	0.00
8	94811972	94811972	TMEM67	A	G	het	n/a	2298	743	I743V	Nonsynonymous (missense)	I/V	absent	0.00
10	128974407	128974407	FAM196A	G	A	het	rs549319983	809	85	R85C	Nonsynonymous (missense)	R/C	0.0001349	0.85
11	33374977	33374977	HIPK3	C	T	het	n/a	3718	1150	R1150C	Nonsynonymous (missense)	R/C	0	0.89
12	105605088	105605088	APPL2	A	G	het	n/a	511	98	L98P	Nonsynonymous (missense)	L/P	absent	0.00
19	13915689	13915689	ZSWIM4	C	T	het	rs375720071	628	147	R147C	Nonsynonymous (missense)	R/C	absent	0.17
19	56538591	56538591	NLRP5	G	T	het	rs369791138	992	331	S331I	Nonsynonymous (missense)	S/I	0.0002152	0.00

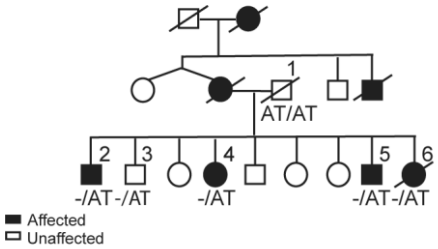

Figure 5. Familial segregation of *BDNF* mutation with schizophrenia. Pedigree of discovery family with schizophrenia. Number 1 to 5 (PED ID) indicate participating individuals. -/AT, heterogzygous carrier of the *BDNF* c.99_100del2 mutation ($BDNF^{Cys34PhefsTer12}$), AT/AT, homozygous reference.

DISCUSSION

Here we report the identification of novel activity-dependent human *BDNF* transcripts in pluripotent stem cell-derived neural lineage cell types. We focused on exon VIII-containing transcripts potentially encoding a prepro-BDNF isoform with a long alternative N-terminus. We show that exon VIII-containing transcripts levels are expressed at low baseline levels in human NPCs, neurons and astrocytes. However, upon KCl-induced depolarization the expression of exon VIII-containing transcripts increased substantially in all three cell types, and most prominently in NPCs. Lastly, we identified a 2-base pair frameshift deletion in *BDNF* exon VIII exhibiting familial co-segregation with SCZ, highlighting the potential functional relevance of human *BDNF* exon VIII-containing transcripts.

We measured *BDNF* transcripts in human pluripotent stem cell derived-NPCs, neurons, and astrocytes. To the best of our knowledge, these results are the first to report the activity-dependent regulation of *BDNF* in human neural lineage cell types. Our findings suggest that human NPCs, neurons, and astrocytes exhibit robust upregulation of *BDNF* expression upon KCl depolarization. The largest increase (over 30-fold upregulation) of exon VIII-containing transcript expression was found in NPCs suggesting that *BDNF* exon VIII-IX transcripts may have a particularly important function during neurodevelopment. Importantly, the strong response in upregulation was confirmed using multiple independent primer sets and in NPCs derived from both ES and iPSC cell lines.

Using primers compatible with detection of both human and mouse exon VIII-containing transcripts, we could not detect *Bdnf* VIII-IX in mouse neuronal lineage cell types. Although Aid et al. 2007 report the presence of *Bdnf* VIII-IX in developing and adult mouse brain[13], we could not detect *Bdnf* VIII-IX expression in either mouse ES-derived NPCs or primary hippocampal mouse neurons. Notably, a recent report also failed to detect *Bdnf* VIII-IX expression in primary hippocampal mouse neurons[24]. However, since Aid et al. 2007 used brain lysates, we cannot exclude that other brain cell types may express *Bdnf* VIII-IX[15]. Species-specific regulation of the other *BDNF* transcripts was also observed. Although several studies report

robust increases of *BDNF* I-IX, IV-IX and VI-IX in rodent neurons upon depolarization[18–20,25], we could detect upregulation of *BDNF* I-IX, IV-IX or VI-IX in human neurons. Although *BDNF* I-IX was undetectable in mouse NPCs, it was present in human NPCs but without evidence of strong activity-dependent regulation. *BDNF* I-IX was undetectable in human astrocytes, both under standard baseline conditions as well as following KCl depolarization. Expression of *BDNF* transcripts IV-IX and VI-IX was activity-dependent, but only in NPCs and astrocytes. Moreover, we observed an unexpected decrease of total *Bdnf* expression in mouse NPCs following KCl depolarization. Overall, these data show marked differences in the regulation of human *BDNF* expression compared to mouse. Earlier results already hinted towards dissimilar time course of upregulation, level of upregulation and relative ratios of transcripts in depolarized and non-depolarized condition between human and mouse cells[18]. Nonetheless, as stem cell-derived cells represent at best first trimester human cells[26,27], *BDNF* transcript expression may be different in more mature neural lineages.

A prior study reported the identification of a human *BDNF* exon V-VIII-IX transcript in adult brain tissue[10,15]. Although we could not detect this transcript in human NPCs, neurons, or astrocytes, we did find expression of three novel human *BDNF* transcripts: *BDNF* IV-VIII-IX, VIa-VIII-IX and VIb-VIII-IX. Taken together, these results suggest that the expression of human *BDNF* transcripts is likely to be neurodevelopmentally-regulated[28], for which transcripts IV-VIII-IX and VI-VIII-IX may predominantly be expressed in the developing brain, while transcript V-VIII-IX is more abundant in the adult brain. Moreover, given the activity-dependent expression of human *BDNF*, it is not unreasonable to presume that additional transcripts may also remain to be identified. For example, given the quadripartite transcript V-VIII-VIIIh-IX[10], IV-VIII-VIIIh-IX and VI-VIII-VIIIh-IX splicing are not unlikely to be found. Moreover, as rodents express a bipartite *Bdnf* VIII-IX transcript, it is possible that human exon VIII may also contain an analogous transcriptional initiation site. *In silico* prediction algorithms indeed annotate the likely existence of human *BDNF* VIII-IX transcripts (XM_011520280.2), but empirical confirmation has not yet been realized.

The function of the various human *BDNF* 5' UTRs remain poorly characterized. In rodents, several 5' UTRs have been shown to influence transcript localization and facilitate localized translation[29–31]. In rats, exon IV-containing transcripts are found in proximal dendrites, whereas exon VI-containing transcripts are targeted to distal dendrites. Exon VIII-containing transcripts remain in the soma[31]. 5' UTRs also influence the amount of protein produced. Several elements in the 5' UTR are involved in regulating translation levels such as secondary structures, multiple open-reading frames, upstream open-reading (uORF) frames and internal ribosomal entry-sites (IRES)[32]. Exon IV, VI and VIII contain several uORFs[33] and IRES sequences[34]. uORFs downregulate expression of the main ORF[35], whereas IRES sequences facilitate translation initiation after the ribosomal complex has disengaged. Of note, exon VIII-containing transcripts have two open-reading frames. Given that the effectivity of an AUG as start-site depends on the context nucleotides surrounding it[36], the in-frame AUG

in exon VIII lies in a weak context for translation initiation[10], whereas the AUG in exon IX occurs within a more classical translation initiation sequence. The mechanisms underlying the post-transcriptional regulation of the various human *BDNF* transcripts remain an important topic to be unraveled further.

Another open question concerns the downstream processing of exon VIII prepro-BDNF protein. ProBDNF contains a highly conserved ER-localization signal (KAAP) that mediates its translocation over the ER membrane[37]. The pro-domain of BDNF also influences packaging and sorting in the Golgi as well as secretion[38–40]. *In silico* prediction by the SignalP 4.1 server[41] does not indicate an ER-localization signal in exon VIII prepro-BDNF. It remains to be determined empirically if the pre-domain of BDNF VIII-IX contains an ER-localization signal and what its effect may be on translocation, the amount of protein synthesized and secreted, sensitivity towards convertases, and where along the secretion path it might be cleaved. Likewise, its ability to form homo or heterodimers with other BDNF protein isoforms, as well as its consequences for secretion, remains to be determined.

Many studies have proposed an association between genetic variation in *BDNF* and SCZ pathophysiology[42,43]. Differential expression of *BDNF* has been reported in postmortem brain tissue and serum of SCZ patients[42,43]. Several antipsychotics appear to alter *BDNF* levels[44]. Moreover, SCZ is widely considered a disease of neurodevelopment[45], in which synaptic dysfunction is a prominent pathophysiological mechanism[46,47]. Extensive findings have demonstrated the critical importance of *BDNF* in synaptic plasticity[2,48–50]. However studies on BDNF and SCZ have yielded inconsistent results[42,43,51,52], leaving open the question of whether and the extent to which variation in *BDNF* might influence SCZ disease risk or its phenotypic manifestation.

We identified a frameshift mutation in the BDNF protein coding part of exon VIII that segregated with SCZ in a Dutch family. However, we did not find enrichment for the mutation in cases in the Swedish Schizophrenia Exome Sequencing Study (dbGAP; phs000473.v1.p1)[23]. Incomplete penetrance of the mutation could be a reason for the lack of enrichment in the Swedish Schizophrenia Exome Sequencing Study. Next to this, severe loss-of-function mutations in *BDNF* are extremely rare (ExAC pLI=0.95)[22]. This indicates that *BDNF* has extreme selective constraints for functional alterations. As such, heterozygous mutation carriers may be at elevated risk for SCZ. Moreover, no homozygous individuals for this alternate allele have yet been found[22]. To prove causality however additional genetic and functional evidence are needed.

In conclusion, in this study we examined the transcriptional regulation of human *BDNF* exon VIII-containing transcripts. We find exon VIII-containing transcripts to be upregulated upon depolarization in human neural cells, particularly NPCs. We identified three novel exon VIII-containing human *BDNF* transcripts and find a loss-of-function mutation in exon VIII exhibiting familial co-segregation with SCZ, suggesting the neurobiological significance of human BDNF exon VIII-containing transcripts.

EXPERIMENTAL PROCEDURES

Cell culture

H9 human embryonic stem cells (hESCs) were maintained on mouse embryonic fibroblasts (MEFs) according to standard protocols[53]. Induced pluripotent stem cells (iPSCs) were reprogrammed from human primary skin fibroblasts (female, age 54) according to Warlich et al. using a single, multicistronic lentiviral vector encoding OCT4, SOX2, KLF4, and MYC[54,55]. The donor provided written informed consent in accordance with the Medical Ethical Committee of the Erasmus University Medical Center. Quality control of iPSC clones was performed by karyotyping, real-time quantitative PCR and embryoid body differentiation[55,56].

Neural progenitor cells (NPCs) were generated according to previous publications[55,57]. In short, ES and induced pluripotent stem cell (iPSC) colonies were dissociated from MEFs with collagenase. IPSC colonies were transferred to non-adherent plates for embryoid body (EB) formation. For two days EBs were grown in human ES medium after which the medium was replaced with neural induction medium for an additional 4 days in suspension. To obtain NPCs, EBs were slightly triturated at day 7 and plated onto laminin-coated 10 cm dishes in neural induction medium for 8 days. At day 15, cells were considered pre-NPCs (passage one, p1). NPCs between p6 and p9 were used for experiments. Neuronal cultures were generated by terminally differentiating p6-9 NPCs according to Gunhanlar et al. 2017[55]. In brief, NPCs were plated on polyornithine/laminin-coated coverslips in neuronal differentiation medium. After 4 weeks of differentiation, only half of the medium of the cultures was replenished. Neuronal cultures were differentiated for 8-10 weeks. For generation of astrocyte cultures, NPCs (p5-p10) were differentiated for 3 weeks in NPC medium supplemented with human LIF (10 ng/ml, Peprotech) and human BMP4 (10 ng/ml, Biovision)[58]. Mouse NPCs were derived from 46C embryonic stem cells [59] and cultured as described in Conti et al. 2005[60]. For mouse primary neuronal cultures, FvB/NHsD females were crossed with FvB/NHsD males (both ordered at 8-10 weeks old from Envigo) and isolated at E18 according Banker and Goslin, 1998[61]. All animal procedures were approved by the local institutional review board and Dutch Animal Ethical Committee.

Quantitative real-time PCR

RNA was isolated from cell cultures using the RNeasy mini kit (Qiagen) or Allprep RNA/protein kit (Qiagen) according manufacturer instructions. RNA quality was assessed with nanodrop (A260/A280>2.0, A260/A230 2.0-2.2) and rRNA was checked with gel electrophoresis for a 28S/18S ratio of 2:1. RNA was stored at -80°C. First-strand cDNA synthesis was performed with the iScript (™) cDNA Synthesis kit (BioRad) according to the manufacturer's protocol with 300 ng RNA template and stored at -20°C. Quantitative RT-PCR primers were designed with Primer Express and Primer3Plus. All primers were blasted and were not homologous to other targets than the one intended. RT-PCR amplification mixtures (20 µl) contained 3-15

ng template cDNA, 7.5 µl 2x Sybr ® Green PCR Master mix (Applied Biosciences), 2.5 µl H_2O and 20 nM forward and reverse primer. For each primer pair a 4-step 2-fold dilution curve was made to check for replication efficiency, except for *GAPDH* where a 10-fold dilution curve was made. Efficiency between 75-100% was measured (**Table S2**). Reactions were run on an ABI 7300 (Applied Biosystems) in microseal PCR plates (MSS9601, Bio-Rad). The cycling conditions comprised 10 min polymerase activation at 95°C, 40 cycles at 95°C for 15 sec, 60°C for 60 sec followed by one cycle of 10 sec at 95°C, 60 sec at 60°C, 15 sec at 95°C, and 60°C for 15 sec. Each assay contained a no-template control, where average ≤ 5 cycle threshold (Ct) cycles was accepted as the threshold. The detection limit was set to Ct=34, above which signals could not be measured reliably. Per plate, three technical replicates were measured. Ct values were determined by automatically determining the threshold and background values using the ABI7300 SDS software (version 1.3). SDS results were exported as tab-delimited text files and imported into Microsoft Excel 2010 for further analysis.

Statistical analysis

Each set of experiments was performed in duplicate in n=3 wells for both treated and non-treated conditions. Delta Ct values (dCt) were determined by subtracting *GAPDH* Ct values from the Ct values of the transcript of interest. Delta dCt (ddCt) values were calculated by subtracting average dCt values in non-treated conditions from each individual dCt value in treated conditions. Delta dCt values were transformed to relative fold change values using the following formula: $2^{(-ddCt)}$. Statistical analysis was performed by unpaired Student *t*-test using Microsoft Excel 2010. Differences were considered statistically significant if the P-value was <0.05.

Immunocytochemistry

Cell cultures were fixed using 4% formaldehyde in PBS. Primary antibodies were incubated overnight at 4°C in labelling buffer containing 0.05 M Tris, 0.9% NaCl, 0.25% gelatin, and 0.5% Triton-X-100 (pH 7.4). The following primary antibodies were used: SOX2, Nestin, MAP2, GFAP (Millipore); secondary antibodies Alexa-488 and Cy3 were used (Jackson ImmunoResearch). Samples were embedded in Mowiol 4-88 (Sigma-Aldrich) after which images were obtained with Zeiss LSM700 confocal microscope using ZEN software (Zeiss, Germany).

Genetic analyses

A non-consanguineous family of Dutch ancestry was identified with a pattern of SCZ inheritance compatible with autosomal dominant transmission. Linkage and copy number variant (CNV) analysis was performed with Illumina HumanOmniExpress 700k SNP-arrays on DNA isolated from venous blood. Linkage analysis was performed using an autosomal dominant affected-only model with an assumption that the pathogenic allele was inherited through the affected mother. Linkage analysis was conducted for the purpose of identifying

the genome-wide set of chromosomal regions shared by all affected family members. This analysis revealed a total of ~407 Mb of shared genomic region (**Table S3**). Linkage analysis was performed using Allegro[62]. CNV analysis was performed using NEXUS discovery edition, version 7 (BioDiscovery, El Segundo, CA). Whole exome sequencing was performed on two affected siblings and their unaffected father (**Figure 8**, PED IDs 1, 2 and 5) at 90x average coverage. Exome sequencing was performed using in-solution capture (Agilent SureSelect V4 Human 50 Mb kit, Agilent Technologies) and paired-end sequencing on an Illumina Hi-Seq 2000 sequencer at LGC Berlin. Reads were aligned to the human reference genome version 19 using Burrows-Wheeler Aligner. SNPs and indels were called using the Genome Analysis Toolkit (GATK). The heterozygous variants were filtered based on the following criteria: a) present within the shared genomic regions, b) predicted to affect protein coding (missense, nonsense, frameshift, splice site), c) called in both affected individuals (Ped IDs 2 and 5) and absent from their unaffected father (Ped ID 1), d) absent from dbSNP129, and e) with a minor allele frequency (MAF) of < 0.1% in public databases 1000G[63], ExAC[22], GoNL[64]. The remaining variants for all participating family members were genotyped by Sanger sequencing (for primers, see **Table S4**).

ACKNOWLEDGEMENTS

We thank Martí Quevedo Calero and Raymond Poot for providing mouse NPCs.

REFERENCES

1. Murer, M., Yan, Q. & Raisman-Vozari, R. Brain-derived neurotrophic factor in the control human brain, and in Alzheimer's disease and Parkinson's disease. *Prog. Neurobiol.* **63**, 71–124 (2001).
2. Panja, D. & Bramham, C. R. BDNF mechanisms in late LTP formation: A synthesis and breakdown. *Neuropharmacology* **76 Pt C**, 664–76 (2014).
3. Zagrebelsky, M. & Korte, M. Form follows function: BDNF and its involvement in sculpting the function and structure of synapses. *Neuropharmacology* **76 Pt C**, 628–38 (2014).
4. Martínez-Levy, G. a & Cruz-Fuentes, C. S. Genetic and epigenetic regulation of the brain-derived neurotrophic factor in the central nervous system. *Yale J. Biol. Med.* **87**, 173–86 (2014).
5. Boulle, F. *et al.* Epigenetic regulation of the BDNF gene: implications for psychiatric disorders. *Mol. Psychiatry* **17**, 584–96 (2012).
6. Castrén, M. L. & Castrén, E. BDNF in fragile X syndrome. *Neuropharmacology* **76 Pt C**, 729–36 (2014).
7. Li, W. & Pozzo-Miller, L. BDNF deregulation in Rett syndrome. *Neuropharmacology* **76 Pt C**, 737–46 (2014).
8. Buckley, P. F., Pillai, A. & Howell, K. R. Brain-derived neurotrophic factor: findings in schizophrenia. *Curr. Opin. Psychiatry* **24**, 122–7 (2011).
9. Autry, A. E. & Monteggia, L. M. Brain-derived neurotrophic factor and neuropsychiatric disorders. *Pharmacol Rev* **64**, 238–258 (2012).
10. Pruunsild, P., Kazantseva, A., Aid, T., Palm, K. & Timmusk, T. Dissecting the human BDNF locus: bidirectional transcription, complex splicing, and multiple promoters. *Genomics* **90**, 397–406 (2007).
11. Yang, B. *et al.* Regional differences in the expression of brain-derived neurotrophic factor (BDNF) propeptide, proBDNF and preproBDNF in the brain confer stress resilience. *Eur. Arch. Psychiatry Clin. Neurosci.* **266**, 1–5 (2016).
12. Anastasia, A. *et al.* Val66Met polymorphism of BDNF alters prodomain structure to induce neuronal growth cone retraction. *Nat. Commun.* **4**, 2490 (2013).
13. Aid, T., Kazantseva, A., Piirsoo, M. & Palm, K. Mouse and Rat BDNF Gene Structure and Expression Revisited. *J of Neuroscience res.* **535**, 525–535 (2007).
14. Baj, G. *et al.* Regulation of the spatial code for BDNF mRNA isoforms in the rat hippocampus following pilocarpine-treatment: A systematic analysis using laser microdissection and quantitative real-time PCR. *Hippocampus* **000**, 1–11 (2013).
15. Herrfurth, N. *et al.* Relevance of polymorphisms in MC4R and BDNF in short normal stature. *BMC Pediatrics* **18:278**, 5–9 (2018).
16. Pruunsild, P., Kazantseva, A., Aid, T., Palm, K. & Timmusk, T. Dissecting the human BDNF locus: bidirectional transcription, complex splicing, and multiple promoters. *Genomics* **90**, 397–406 (2007).
17. Vaghi, V. *et al.* Pharmacological Profile of Brain-Derived Neurotrophic Factor (BDNF) Splice Variants Translation Using a Novel Drug Screening Assay: a "Quantitative Code". *J. Biol. Chem.* (2014). doi:10.1074/jbc.M114.586719
18. Pruunsild, P., Sepp, M., Orav, E., Koppel, I. & Timmusk, T. Identification of cis-elements and transcription factors regulating neuronal activity-dependent transcription of human BDNF gene. *J. Neurosci.* **31**, 3295–308 (2011).
19. Marmigère, F., Rage, F. & Tapia-Arancibia, L. Regulation of brain-derived neurotrophic factor transcripts by neuronal activation in rat hypothalamic neurons. *J. Neurosci. Res.* **66**, 377–89 (2001).
20. Koppel, I. *et al.* Tissue-specific and neural activity-regulated expression of human BDNF gene in BAC transgenic mice. *BMC Neurosci.* **10**, 68 (2009).

21. Pardiñas, A. F. *et al.* Common schizophrenia alleles are enriched in mutation-intolerant genes and in regions under strong background selection. *Nat. Genet.* **50**, 381–389 (2018).
22. Lek, M. *et al.* Analysis of protein-coding genetic variation in 60,706 humans. *Nature* **536**, 285–291 (2016).
23. Purcell, S. M. *et al.* A polygenic burden of rare disruptive mutations in schizophrenia. *Nature* **506**, 185–190 (2014).
24. Rousseaud, A., Delépine, C., Nectoux, J., Billuart, P. & Bienvenu, T. Differential Expression and Regulation of Brain-Derived Neurotrophic Factor (BDNF) mRNA Isoforms in Brain Cells from Mecp2308/y Mouse Model. *J. Mol. Neurosci.* **56**, 758–767 (2015).
25. Tao, X., Finkbeiner, S., Arnold, D. B., Shaywitz, A. J. & Greenberg, M. E. Ca2+ influx regulates BDNF transcription by a CREB family transcription factor-dependent mechanism. *Neuron* **20**, 709–726 (1998).
26. Mariani, J., Vittoria, M., Palejev, D. & Tomasini, Livia; Coppola, G.; Szekely, A.M.; Horvath, T.L.; Vaccarino, M. V. Modeling human cortical development in vitro using induced pluripotent stem cells. *Proc. Natl. Acad. Sci.* **109**, 12770–12775 (2012).
27. van de Leemput, J. *et al.* CORTECON: A Temporal Transcriptome Analysis of In Vitro Human Cerebral Cortex Development from Human Embryonic Stem Cells. *Neuron* **83**, 51–68 (2014).
28. Wong, J., Webster, M. J., Cassano, H. & Weickert, C. S. Changes in alternative brain-derived neurotrophic factor transcript expression in the developing human prefrontal cortex. *Eur. J. Neurosci.* **29**, 1311–22 (2009).
29. Chiaruttini, C., Sonego, M., Baj, G., Simonato, M. & Tongiorgi, E. BDNF mRNA splice variants display activity-dependent targeting to distinct hippocampal laminae. *Mol. Cell. Neurosci.* **37**, 11–9 (2008).
30. Pattabiraman, P. P. *et al.* Neuronal activity regulates the developmental expression and subcellular localization of cortical BDNF mRNA isoforms in vivo. *Mol. Cell. Neurosci.* **28**, 556–70 (2005).
31. Baj, G., Leone, E., Chao, M. V & Tongiorgi, E. Spatial segregation of BDNF transcripts enables BDNF to differentially shape distinct dendritic compartments. *Proc. Natl. Acad. Sci. U. S. A.* **108**, 16813–8 (2011).
32. Mignone, F., Gissi, C., Liuni, S. & Pesole, G. Untranslated regions of mRNAs. *Genome Biology* **vol 3 No 3**, 1–10 (2002).
33. Pedersen, A. G. & Nielsen, H. Neural network prediction of translation initiation sites in eukaryotes: perspectives for EST and genome analysis. *Proceedings. Int. Conf. Intell. Syst. Mol. Biol.* **5**, 226–33 (1997).
34. Grillo, G. *et al.* UTRdb and UTRsite (RELEASE 2010): a collection of sequences and regulatory motifs of the untranslated regions of eukaryotic mRNAs. *Nucleic Acids Res.* **38**, D75–D80 (2010).
35. Kidane, A. H. *et al.* Differential neuroendocrine expression of multiple brain-derived neurotrophic factor transcripts. *Endocrinology* **150**, 1361–1368 (2009).
36. Kozak, M. Point mutations define a sequence flanking the AUG initiator codon that modulates translation by eukaryotic ribosomes. *Cell* **44**, 283–292 (1986).
37. Tettamanti, G. *et al.* Phylogenesis of brain-derived neurotrophic factor (BDNF) in vertebrates. *Gene* **450**, 85–93 (2010).
38. Egan, M. F. *et al.* The BDNF val66met polymorphism affects activity-dependent secretion of BDNF and human memory and hippocampal function. *Cell* **112**, 257–69 (2003).
39. Jiang, X., Zhou, J., Mash, D. C., Marini, A. M. & Lipsky, R. H. Human BDNF isoforms are differentially expressed in cocaine addicts and are sorted to the regulated secretory pathway independent of the Met66 substitution. *Neuromolecular Med.* **11**, 1–12 (2009).
40. Koppel, I., Tuvikene, J., Lekk, I. & Timmusk, T. Efficient use of a translation start codon in BDNF exon I. *J. Neurochem.* n/a-n/a (2015). doi:10.1111/jnc.13124

41. Petersen, T. N., Brunak, S., Heijne, G. Von & Nielsen, H. correspondEnce SignalP 4 . 0 : discriminating signal peptides from transmembrane regions. *Nat. Publ. Gr.* **8**, 785–786 (2011).
42. Favalli, G., Li, J., Belmonte-de-Abreu, P., Wong, A. H. C. & Daskalakis, Z. J. The role of BDNF in the pathophysiology and treatment of schizophrenia. *J. Psychiatr. Res.* **46**, 1–11 (2012).
43. Nieto, R., Kukuljan, M. & Silva, H. BDNF and schizophrenia: from neurodevelopment to neuronal plasticity, learning, and memory. *Front. Psychiatry* **4**, 45 (2013).
44. L. Huang, T. Effects of Antipsychotics on the BDNF in Schizophrenia. *Curr. Med. Chem.* **20**, 345–350 (2013).
45. Ross, C. A., Margolis, R. L., Reading, S. A. J., Pletnikov, M. & Coyle, J. T. Neurobiology of Schizophrenia. *Neuron* **52**, 139–153 (2006).
46. Wang, X., Christian, K. M., Song, H. & Ming, G. li. Synaptic dysfunction in complex psychiatric disorders: From genetics to mechanisms. *Genome Med.* **10**, 9–11 (2018).
47. Osimo, E. F., Beck, K., Reis Marques, T. & Howes, O. D. Synaptic loss in schizophrenia: a meta-analysis and systematic review of synaptic protein and mRNA measures. *Mol. Psychiatry* 1–13 (2018). doi:10.1038/s41380-018-0041-5
48. Lu, B., Pang, P. T. & Woo, N. H. The yin and yang of neurotrophin action. *Nat. Rev. Neurosci.* **6**, 603–614 (2005).
49. Leal, G., Comprido, D. & Duarte, C. B. BDNF-induced local protein synthesis and synaptic plasticity. *Neuropharmacology* **76 Pt C**, 639–56 (2014).
50. Lu, B. BDNF and Activity-Dependent Synaptic Modulation. *Learning & Memory* **10**, 86-98 (2003)
51. Cui, H., Jin, Y., Wang, J., Weng, X. & Li, C. Serum brain-derived neurotrophic factor (BDNF) levels in schizophrenia : A systematic review. *Shanghai Arch. of Psychiatry* **24**, 250–261 (2012).
52. Green, M. J., Matheson, S. L., Shepherd, A., Weickert, C. S. & Carr, V. J. Brain-derived neurotrophic factor levels in schizophrenia : a systematic review with meta-analysis. *Mol. Psychiatry* **16**, 960–972 (2010).
53. Cowan, C. A. *et al.* Derivation of Embryonic Stem-Cell Lines from Human Blastocysts. N Engl J Med 350:13 1353–1356 (2004).
54. Warlich, E. *et al.* Lentiviral Vector Design and Imaging Approaches to Visualize the Early Stages of Cellular Reprogramming. *Mol. Ther.* **19**, 782–789 (2011).
55. Gunhanlar, N. *et al.* A simplified protocol for differentiation of electrophysiologically mature neuronal networks from human induced pluripotent stem cells. *Mol. Psychiatry* 1–9 (2017). doi:10.1038/mp.2017.56
56. De Esch, C. E. F. *et al.* Epigenetic characterization of the FMR1 promoter in induced pluripotent stem cells from human fibroblasts carrying an unmethylated full mutation. *Stem Cell Reports* **3**, 548–555 (2014).
57. de Vrij, F. M. *et al.* Candidate CSPG4 mutations and induced pluripotent stem cell modeling implicate oligodendrocyte progenitor cell dysfunction in familial schizophrenia. *Mol. Psychiatry* 1–15 (2018).
58. Kondo, T. *et al.* Modeling Alzheimer's disease with iPSCs reveals stress phenotypes associated with intracellular Aβ and differential drug responsiveness. *Cell Stem Cell* **12**, 487–96 (2013).
59. Ying, Q.-L., Stavridis, M., Griffiths, D., Li, M. & Smith, A. Conversion of embryonic stem cells into neuroectodermal precursors in adherent monoculture. *Nat. Biotechnol.* **21**, 183–6 (2003).
60. Conti, L. *et al.* Niche-independent symmetrical self-renewal of a mammalian tissue stem cell. *PLoS Biol.* **3**, 1594–1606 (2005).
61. Banker, G. & Goslin, K. Culturing nerve cells. *Cambridge MA MIT Press* (1991).
62. Lindner, T. H. & Hoffmann, K. easyLINKAGE: A PERL script for easy and automated two-/multi-point linkage analyses. *Bioinformatics* **21**, 405–407 (2005).

63. Abecasis GR. A map of human genome variation from population-scale sequencing. *Nature* **467**, 1061–73 (2010).
64. The Genome of the Netherlands Consortium. Whole-genome sequence variation, population structure and demographic history of the Dutch population. *Nat. Genet.* **46**, 1–95 (2014).

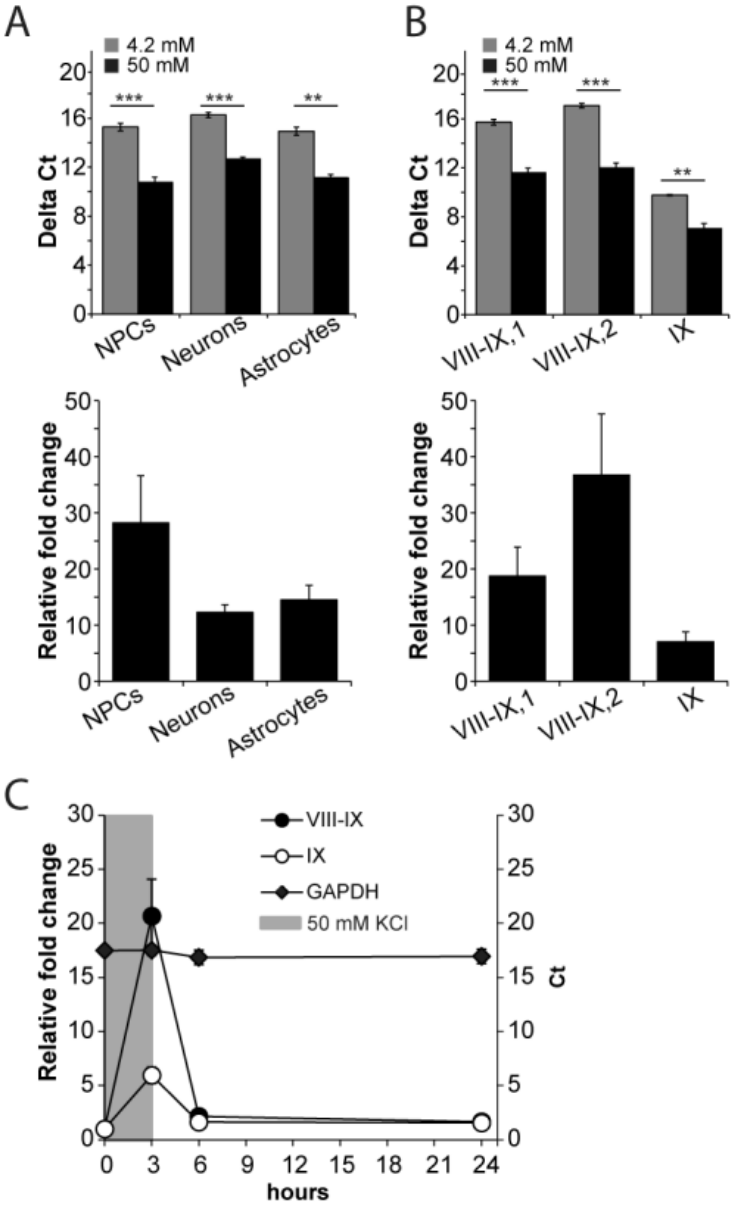

Figure S1. Validation of *BDNF* VIII-IX upregulation (A) ES-derived NPCs, neuronal cultures and astrocytes and (B) iPSC-derived NPCs were treated for 3hs with 50 mM KCl and *BDNF* transcript VIII-IX and IX were measured by qRT-PCR using transcript-specific primers, normalized to *GAPDH*. Delta Ct values and relative fold change values are shown. Relative fold change values are calculated with respect to untreated cultures. (C) NPCs were treated for 3hs with 50 mM KCl after which the medium was replaced with fresh medium. *BDNF* VIII-IX and IX levels were measured 3hs and 18hs after replenishment. Fold changes are relative to untreated cultures. The *GAPDH* Ct values stay constant over time. Error bars represent SEM. Statistical significance is denoted by asterisks (***p<0.001; **p<0.01; *p<0.05; NS; Student *t*-test, ANOVA).

Table S1, Related to figure 4, relative fold change and dCt values

		Relative fold change	dCt treated cultures	dCt untreated cultures	P-value
NPCs	IV-IX	4.94 ± 0.56	8.26 ± 0.16	10.53 ± 0.12	1.04E-06
	IV-VIII	7.94 ± 1.52	13.71 ± 0.27	16.57 ± 0.36	8.26E-05
	VI-XI	4.08 ± 0.56	8.40 ± 0.30	10.32 ± 0.12	1.41E-04
	VIa-VIII	11.67 ±2.32	12.68 ± 0.25	16.10 ± 0.13	2.86E-07
	VIb-VIII	21.69 ± 5.85	11.21 ± 0.47	15.31 ± 0.33	3.15E-05
Neurons	IV-IX	1.78 ± 0.43	9.00 ± 0.40	9.68 ± 0.39	3.48E-01
	IV-VIII	3.02 ± 0.76	14.51 ± 0.37	15.83 ± 0.46	4.96E-02
	VI-XI	2.27 ± 0.54	10.93 ± 0.31	12.01 ± 0.91	2.13E-01
	VIa-VIII	5.07 ± 2.63	13.86 ± 0.68	15.20 ± 0.18	1.34E-01
	VIb-VIII	4.32 ± 1.16	12.65 ± 0.34	14.51 ± 0.43	6.39E-03
Astrocytes	IV-IX	5.99 ± 1.76	10.16 ± 0.51	12.34 ± 0.68	2.81E-02
	IV-VIII	4.08 ± 1.14	13.37 ± 0.46	15.27 ± 0.23	2.06E-02
	VI-XI	1.82 ± 0.16	8.41 ± 0.30	10.32 ± 0.12	7.29E-03
	VIa-VIII	14.53 ± 5.04	12.45 ± 0.74	15.58 ± 0.12	1.83E-03
	VIb-VIII	14.53 ± 5.31	12.34 ± 0.61	15.61 ± 0.10	3.68E-04

Table S2, Related to Figure 2, 3, 4, primers for different BDNF isoforms

	Transcript	Forward primer	Reverse primer	Efficiency (%)
Human	BDNF I-IX	CAGCATCTGTTGGGGAGACGAGA	ATGGGGGCAGCCTTCATGCA	91
	BDNF IV-IX	AGTGACTGAAAAGTTCCACCAG	GTAGGCCAAGCCACCTTGT	98
	BDNF VI-IX	ACCCGTGAGTTCCACCAG	GTAGGCCAAGCCACCTTGT	82
	BDNF IV-VIII-IX	CGAAGTCTTTCCCGGAGCAG	TGGCTCCACACATCCAGTTG	76
	BDNF VIa-VIII-IX	GGACCCGTGAGTTAAGTAATTAAAAG	GGAGAAAACTGGTGGCTCCA	92
	BDNF VIb-VIII-IX	GGTTTGTGTGGACCCCGAG	GGAGAAAACTGGTGGCTCCA	89
	BDNF VIII-IX, primer pair 1	AAGGGCTGTGCTGTGTACCTCC	TGGTCATCACTCTTCTCACCTGG	101
	BDNF VIII-IX, primer pair 2	TGTGCATCCCAGAAGAAGG	CTGGTGGAACTTTATGAAACCA	89
	BDNF VIII-IX, common mouse human	TAACCCGAAGGACAACTGGA	AAGGATGGTCATCACTCTTCTCA	91
	BDNF IX	AGTGCCGAACTACCCAGTCGTA	CTTATGAATCGCCAGCCAATTC	106
	GAPDH	TGCACCACCAACTGCTTAGC	GGCATGGACTGTGGTCATGAG	117
Mouse	BDNF I-IX	AGTCTCCAGGACAGCAAAGC	GCCTTCATGCAACCGAAGTA	103
	BDNF VIII-IX, common mouse human	TAACCCGAAGGACAACTGGA	AAGGATGGTCATCACTCTTCTCA	91
	BDNF IX	TTGTTTTGTGCCGTTTACCA	TGTGATGGGGATCCTTTTGT	89
	Gapdh	TGCACCACCAACTGCTTAGC	GGCATGGACTGTGGTCATGAG	117

Table S3, Related to Figure 5, shared chromosomal regions under an autosomal dominant, affected-only model

Chr.	Start SNP	End SNP	cM Start	cM End	Physical start	Physical End	Size cM	Size Mb
2	rs870638	rs12469652	44.95	61.07	21484754	36977116	16.12	15.49
3	rs6799673	rs11707471	56.87	69.71	31701082	46498865	12.84	14.80
4	rs3829	rs4637403	0.16	17.89	134851	7554721	17.73	7.42
4	rs1463842	rs7671645	51.07	56.8	31209875	38019302	5.73	6.81
4	rs1433418	rs4693933	73.82	95.88	58984954	89139002	22.06	30.15
4	rs4416516	rs17080259	187.87	205.06	184783233	190838050	17.19	6.05
5	rs12658051	rs11958855	81.1	119.32	68003457	113641145	38.22	45.64
5	rs265993	rs2287716	194.59	206.25	174846909	180666276	11.66	5.82
7	rs6950505	rs6462017	21.76	43.43	11033756	27516318	21.67	16.48
8	rs2003497	rs1915418	0.26	32.73	176818	19093006	32.47	18.92
8	rs4363185	rs12681417	86.98	112.22	74275261	105635003	25.24	31.36
9	rs10814410	rs10810110	0.01	28.4	46587	14199422	28.39	14.15
9	rs3780136	rs12684856	58.63	74.31	36845973	79818630	15.68	42.97
10	rs1772810	rs6537616	137.81	179.57	119157485	135428246	41.76	16.27
11	rs1484444	rs697315	23.98	52.36	15752803	35638772	28.38	19.89
11	rs2000605	rs4945383	76.69	86.25	70353848	79598935	9.56	9.25
12	rs10879636	rs2268389	87.11	124.4	73961218	109643152	37.29	35.68
14	rs1307538	rs12589785	56.22	69.66	56920207	71690700	13.44	14.77
15	rs6599770	rs11632150	3.95	44.28	20161372	46052390	40.33	25.89
17	rs11656081	rs2587507	117.76	129.41	75222048	77790135	11.65	2.57
19	rs475112	rs2886790	12.81	37.08	3745546	15099441	24.27	11.35
19	rs8108275	rs893185	92.59	110.92	53141566	58989495	18.33	15.49
						Total	490.01	407.23

Table S4, Related to Figure 5, sanger sequencing primers

Chr	Start	End	Gene	Amino acid change	Forward primer	Reverse primer
11	27695731	27695733	BDNF	C34PhefsTer12	GCTGGGAGCTGGGGTAGAGC	TGCCTCTAGAGACCAAAGAATAACACTCC
4	1348905	1348905	UVSSA	R350C	GCAGCTTTGTCCTCTGCATCC	AGCTGCACTGTCCCCTCTGC
5	86703854	86703854	CCNH	N155T	AACAATTCTTGCAATGTCTAGCAGTC	CAGGCCAGACCCACAGGTTG
8	17503464	17503464	MTUS1	F509L	CAATGGGGACCTGTGTAGCC	TGAAAAAGGCAATGAACAAGATGC
8	94811972	94811972	TMEM67	I743V	TTTTTCAAGGTGAGTAGGGAGAGG	TTCTGCTACAGAAAGAAGGATGTGG
10	128974407	128974407	FAM196A	R85C	GTGCAGTTGACCCCCAAAGG	CCTGCAGGTGCGGTTTAAGG
11	33374977	33374977	HIPK3	R1150C	TGGGCATCAAGAGTGGAATGG	TGGATACTGGCTGAGTTTTGTTGG
12	105605088	105605088	APPL2	L98P	GGCATTTCTCAGCGATCCACA	GGCCCAGAGTGGGAACACAG
19	13915689	13915689	ZSWIM4	R147C	AGTGACTCGGCTGGGCTTTG	AGCTGGTCCCGGTTCATCTG
19	56538591	56538591	NLRP5	S331I	AAACGTTGGCTGGTGCTTTTG	TGAACGGAGGCTGCTTCTCAG